

# Exact results of two-component ultra-cold Fermi gas in a hard wall trap

Bo-Bo Wei<sup>1</sup>, Jun-Peng Cao<sup>1,2</sup>, Shi-Jian Gu<sup>1</sup>, and Hai-Qing Lin<sup>1</sup>

<sup>1</sup> *Department of Physics and Institute of Theoretical Physics,  
The Chinese University of Hong Kong, Hong Kong, China*

<sup>2</sup> *Beijing National Laboratory for Condensed Matter Physics,  
Institute of Physics, Chinese Academy of Sciences, Beijing 100190, China*

(Dated: July 14, 2008)

The ground state properties of a one-dimensional two-component ultra-cold Fermi gas in an infinite potential well are investigated. The wave function of the system is obtained explicitly based on the solution of Bethe ansatz equations. The single-particle reduced density matrix and two-particle density-density correlations are also evaluated. It is found that the momentum density distributions of the strongly interacting two-component Fermi gas is significantly different from that of free spinless Fermi gas while the density distributions in real space are similar.

PACS numbers: 05.30.Fk, 67.85.-d, 71.10.-w

## I. INTRODUCTION

There have been remarkable experimental advancements in the area of trapped one-dimensional cold atom systems [1, 2, 3, 4]. The one-dimensional quantum gas can be realized experimentally by tightly confining the atomic cloud in the radial directions and weakly confining it along the axial direction [5, 6]. Since the radial degrees of freedom are frozen [7, 8], the quantum gas can be effectively described by a one-dimensional model along the axial direction. Using Feshbach resonance, the energy of a bound state of two colliding atoms in a magnetic field was tuned to vary the scattering length from  $-\infty$  to  $\infty$ , which allows experimental access to strongly interacting regime and studying the crossover from a BCS to Bose-Einstein Condensation. [9, 10, 11, 12]. The experimental achievements have opened up many exciting possibilities for theoretical investigation of quantum effects in low-dimensional many-body systems.

Exactly solvable models provide us an important insight in studying the quantum many-body physics beyond various approximation schemes. The exact solutions can supply some believable results thus serve as a very good starting point to understand the new phenomena and new quantum states in trapped cold atomic systems. Recently, the study of one-dimensional bosons with contact interactions in an infinite potential well shows a revival of interest [13, 14]. We note that the point-interacting two-component Fermi gas in a hard wall trap is also interesting. Many new physics appears in the fermionic system and most important is that this system is integrable [15, 16, 17, 18, 19]. Meanwhile, this systems can be realized in experiment by the laser cooling technique.

In this paper, we investigate the one-dimensional ultra-cold two-component Fermi gas in an infinite potential well. Most of the previous studies focus on the energy spectrum and its related quantities. Here, we put our attentions on the wave function of the system. We study the single-particle reduced density matrix, natural orbitals, the momentum density distributions and two-

body correlations based on the exact wave function of the system. These quantities are important for a better understanding of the ground state properties of the fermion system and can be detected in experiments directly.

The paper is organized as follows. In Sec. II, the model Hamiltonian and its Bethe-ansatz solution are introduced in details. In Sec. III, we study the one-body aspects of correlations. Specifically, we present single-particle reduced density matrix in the context of long range order in Sec.IIIA. In Sec. IIIB, We discuss the natural orbitals and their populations. The momentum density distributions are shown in Sec. IIIC. In Sec. IV, we go further to study the two particle correlations. A summary of our main results is given in Sec. V.

## II. THE MODEL AND ITS EXACT SOLUTION

We consider a system of two-component Fermi gas with  $\delta$  interaction confined in one-dimensional box of length  $L$ . The model Hamiltonian reads

$$\mathcal{H} = - \sum_{i=1}^N \frac{\partial^2}{\partial x_i^2} + 2c \sum_{i<j}^N \delta(x_i - x_j), \quad (1)$$

where  $c$  is the interaction strength between different spins of fermions and  $N$  is total number of fermions. The coupling  $c$  can be expressed in terms of the scattering length as  $c = 2/a_{1D}$ , where  $a_{1D}$  is the effective one-dimensional scattering length. The  $c = 0$  and  $c \rightarrow \infty$  limits correspond to zero and infinite interactions, respectively. It can be tuned by the scattering length. The coupling is repulsive for  $c > 0$  and attractive for  $c < 0$ . We only consider the repulsive case in this work. We introduce another important parameter  $\gamma$  that characterizes the different physical regimes of one-dimensional quantum gas,  $\gamma = c/\rho$  where  $\rho = N/L$  denotes the linear density of the system.

The wave function of system (1) is antisymmetric, and can be characterized by the total number

of fermions  $N$  and the number of spin-down fermions  $M$ . Suppose the antisymmetric wave function is  $\Psi(x_1\sigma_1, x_2\sigma_2, \dots, x_N\sigma_N)$ , where  $x_j$  and  $\sigma_j$  are the position coordinates and spin coordinates of  $j$ -th fermion, respectively. Then the static Schrödinger equation for the wave function  $\Psi$  reads [20]:

$$\left( -\sum_{i=1}^N \frac{\partial^2}{\partial x_i^2} + 2c \sum_{1 \leq i < j \leq N} \delta(x_i - x_j) \right) \Psi = E\Psi. \quad (2)$$

The explicit form of the wave function of the system in region  $x_{Q_1} \leq x_{Q_2} \leq \dots \leq x_{Q_N}$  reads [17]

$$\begin{aligned} & \Psi(x_1\sigma_1, x_2\sigma_2, \dots, x_N\sigma_N) \\ &= \sum_{P, r_1, \dots, r_N} (-1)^P (-1)^Q A_{\sigma_{Q_1}, \dots, \sigma_{Q_N}}(r_1 k_{p_1}, \dots, r_N k_{p_N}) \\ & \times \exp(i \sum_j r_j k_{p_j} x_j). \end{aligned} \quad (3)$$

Here  $P$  and  $Q$  are permutations of  $1, 2, \dots, N$  and  $r_j = \pm 1$  indicate whether the particles move right or left. The function  $A_{\sigma_{Q_1}, \dots, \sigma_{Q_N}}(r_1 k_{p_1}, \dots, r_N k_{p_N})$  is given as

$$\begin{aligned} & A_{\sigma_{Q_1}, \dots, \sigma_{Q_N}}(r_1 k_{p_1}, \dots, r_N k_{p_N}) \\ &= \sum_{q, \epsilon_\alpha = \pm 1} S(\epsilon_{q_1} \Lambda_{q_1}, \dots, \epsilon_{q_M} \Lambda_{q_M}) \\ & \times \prod_{\alpha=1}^M F_{r_1 k_{p_1}, \dots, r_N k_{p_N}}(\epsilon_{q_\alpha} \Lambda_{q_\alpha}; m_\alpha), \end{aligned} \quad (4)$$

with  $m_\alpha$  being the indices of the  $M$  down spins in an increasing order ( $m_\alpha < m_{\alpha+1}$ ),  $q$  denotes the permutations of  $1, 2, \dots, M$ , and  $\sum_q$  means the summation over all the permutations. The functions  $F$  are

$$F_{k_1, \dots, k_N}(\Lambda; m) = \prod_{j=1}^{m-1} \frac{k_j - \Lambda + ic/2}{k_j - \Lambda - ic/2} \frac{1}{k_m - \Lambda - ic/2}, \quad (5)$$

while the coefficients  $S$  are determined by the equations

$$\frac{S(\dots, \Lambda_\alpha, \Lambda_\beta, \dots)}{S(\dots, \Lambda_\beta, \Lambda_\alpha, \dots)} = \frac{\Lambda_\beta - \Lambda_\alpha + ic}{\Lambda_\beta - \Lambda_\alpha - ic}. \quad (6)$$

The hard wall boundary condition sets the requirement of the wave function as,

$$\Psi(0\sigma_1, \dots, x_N\sigma_N) = \Psi(x_1\sigma_1, \dots, L\sigma_N) = 0. \quad (7)$$

The eigenvalue equation (3) can then be solved by the coordinate Bethe ansatz method [16]. The eigenenergy is given by

$$E = \sum_{j=1}^N k_j^2, \quad (8)$$

where the quasimomenta  $k_j$  should satisfy the Bethe ansatz equations [17, 18]

$$\begin{aligned} k_j L &= \pi I_j - \sum_{\beta=1}^M \left( \arctan \frac{k_j - \Lambda_\beta}{c/2} + \arctan \frac{k_j + \Lambda_\beta}{c/2} \right), \\ \sum_{j=1}^N \left( \arctan \frac{\Lambda_\alpha - k_j}{c/2} + \arctan \frac{\Lambda_\alpha + k_j}{c/2} \right) &= \pi J_\alpha \\ &+ \sum_{\beta=1}^M \left( \arctan \frac{\Lambda_\alpha - \Lambda_\beta}{c} + \arctan \frac{\Lambda_\alpha + \Lambda_\beta}{c} \right). \end{aligned} \quad (9)$$

Here  $j = 1, 2, \dots, N$  and  $\alpha = 1, 2, \dots, M$ , where  $M$  is the number of the spin-down fermions. The two sets of variables  $\{k_j\}$  and  $\{\Lambda_\alpha\}$  are the quasi-momenta and spin rapidities, respectively.  $\{I_j\}$  and  $\{J_\alpha\}$  are quantum numbers. For the ground state, the quantum number configuration is described by a continuous sequence:

$$\begin{aligned} I_j &= j, 1 \leq j \leq N; \\ J_\alpha &= \alpha, 1 \leq \alpha \leq M. \end{aligned}$$

The values of quasi-momenta and the explicit form of the wave function are determined by the solutions of the Bethe ansatz equations (9). In the case where the interactions among the atoms are repulsive, we have two interesting limiting regimes. One is two-component free Fermi gas and the other is infinite repulsion interaction case which is like the case of indistinguishable spinless fermions.

If  $c = 0$ , the system (1) degenerates to the noninteracting two-component Fermi gas. The quasi-momentum takes the value of the real momentum and the fermions occupy the single particle momentum states according to the Pauli exclusion principle. The wave function of  $N$  noninteracting fermions with  $M$  spin-down fermions is given by the Slater determinant as:

$$\Psi = \det \begin{pmatrix} \psi_1(x_1 \uparrow) & \dots & \dots & \psi_1(x_N \uparrow) \\ \psi_1(x_1 \downarrow) & \dots & \dots & \psi_1(x_N \downarrow) \\ \psi_2(x_1 \uparrow) & \dots & \dots & \psi_2(x_N \uparrow) \\ \vdots & \vdots & \ddots & \vdots \\ \psi_{N-M}(x_1 \uparrow) & \dots & \dots & \psi_{N-M}(x_N \uparrow) \end{pmatrix}. \quad (10)$$

where  $\psi_m = \sqrt{\frac{2}{L}} \sin(\frac{m\pi}{L})$ ,  $m = 1, 2, \dots, N$  is the single-particle eigenstates of a particle in an infinite potential.

If  $c \rightarrow \infty$ , the system (1) degenerates to the spinless fermions. The fermions cannot feel  $\delta$  interaction of each other as the wave function must vanishes when two spinless fermions touch each other, so the atoms must occupy the single particle momentum eigenstates with momenta  $k_j = \frac{2\pi}{L} (j = 1, 2, \dots, N)$ . The anti-symmetric wave function for the  $N$  spinless fermions is

$$\Psi = \det \begin{pmatrix} \psi_1(x_1) & \psi_1(x_2) & \dots & \psi_1(x_N) \\ \psi_2(x_1) & \psi_2(x_2) & \dots & \psi_2(x_N) \\ \psi_3(x_1) & \psi_3(x_2) & \dots & \psi_3(x_N) \\ \vdots & \vdots & \ddots & \vdots \\ \psi_N(x_1) & \psi_N(x_2) & \dots & \psi_N(x_N) \end{pmatrix}. \quad (11)$$

### III. SINGLE-PARTICLE DISTRIBUTION

#### A. Single-particle reduced density matrix and off-diagonal long range order

In quantum mechanics, the density matrix  $\rho_N = |\Psi\rangle\langle\Psi|$  plays an important role. We first consider the single-particle reduced density matrix

$$\rho_1 = \text{Tr}_{23\dots N} |\Psi\rangle\langle\Psi|, \quad (12)$$

where the trace means to do integrations over all the position coordinates and spin indices except one of them as we are considering the spin-half particle system. In coordinate representation, it is given by

$$\rho_1(x, x') = \frac{N \int_0^L \Psi^*(x, x_2, \dots, x_N) \Psi(x', x_2, \dots, x_N) dx_2 \dots dx_N}{\int_0^L |\Psi(x_1, x_2, \dots, x_N)|^2 dx_1 \dots dx_N}.$$

The diagonal matrix elements  $\rho(x, x)$  give the real space position density distribution of the particles, which are shown in Fig. 1. Starting from noninteracting case  $c = 0$ , where the fermions occupy the single-particle momentum states, the position density is the sum of the  $N$  independent fermions lying in their own momentum states according to the Pauli exclusion principle. When interaction strength increases, the distributions are smoothened, and the half-width increases gradually. As the interaction increases further, the position density distribution tends to that of the spinless fermions.

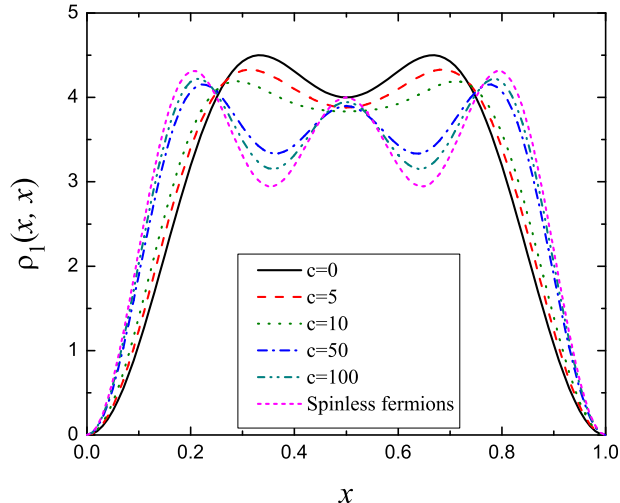


FIG. 1: (color online) Position density distributions of fermions with different interactions for  $N = 3, M = 1$ .

The off-diagonal matrix elements show the correlations between particles at different positions which come from

quantum fluctuations. The single-particle reduced density matrix is shown in Fig. 2 for different repulsive interactions. The single-particle reduced density matrix expresses the self-correlations for a single particle in real space. In classical mechanics, it is a Dirac delta function  $\delta(x - x')$ . So one can observe from Fig. 1 that a strong enhancement of  $\rho(x, x')$  exists along the diagonal line  $x = x'$  for all interaction strengths.

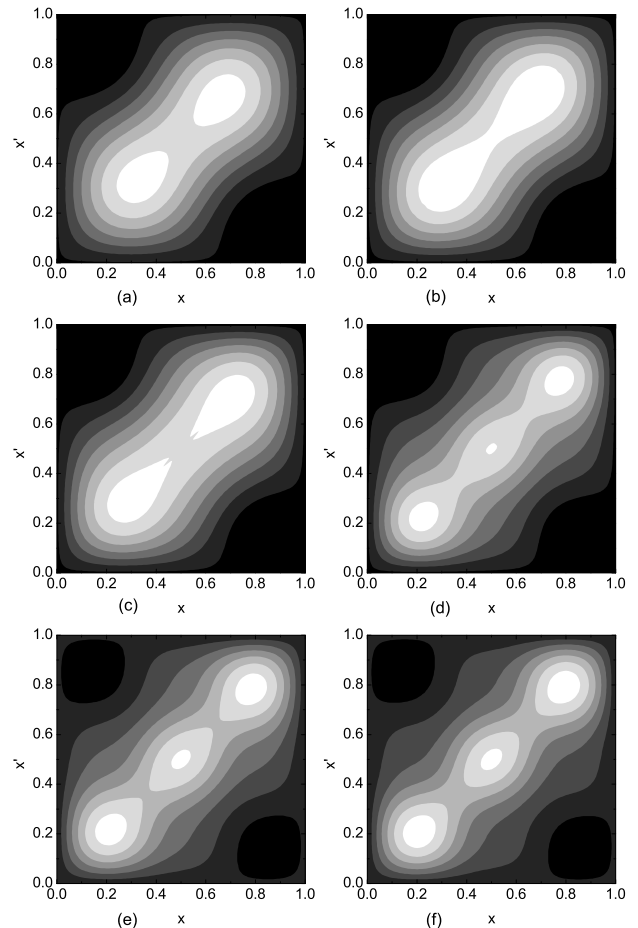


FIG. 2: Single-particle reduced density matrix  $\rho(x, x')$  as a function of interaction strength for  $N = 3, M = 1$ . Shown are the interactions (a)  $c = 0$ , (b)  $c = 5$ , (c)  $c = 10$ , (d)  $c = 50$ , (e)  $c = 100$  and (f)  $c = 1000$ .

#### B. Natural orbitals and their populations

The spectral decomposition of the single-particle reduced density matrix gives

$$\int dx' \rho_1(x, x') \phi_i(x') = \lambda_i \phi_i(x), \quad i = 1, 2, \dots, \quad (13)$$

where  $\phi_i(x)$  are the so called natural orbitals, which is obtained from the eigenfunctions of the single-particle

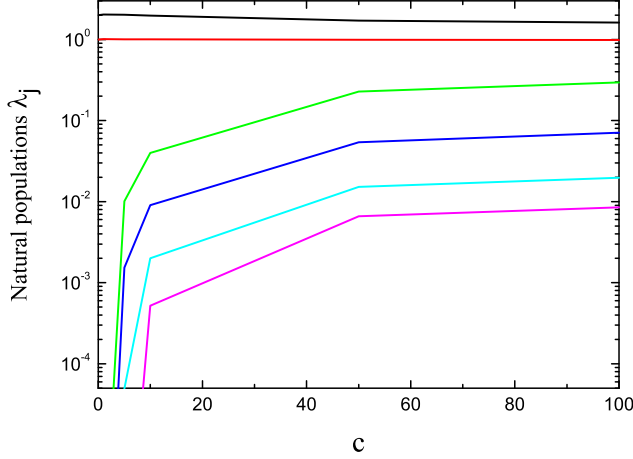


FIG. 3: (color online). Evolution of the populations of the six lowest natural orbitals  $\phi_i$  with the interactions for the case of  $N = 3, M = 1$ .

reduced density matrix and represents an effective single-particle states, and  $\lambda_i$  is population of the  $i$ -th natural orbital and satisfies  $\sum_i \lambda_i = N$ .

We first consider two limit cases. For noninteracting two-component Fermi gas, the single-particle wave functions  $\psi_i(x)$  are the natural orbitals of the system and  $\lambda_j = 2$ , for  $j = 1, 2, \dots, M$  and  $\lambda_j = 1$ , for  $j = M + 1, \dots, N - M$ , all the higher eigenvalues being zero as their reduced density matrix can be given as

$$\rho_1(x, x') = 2 \sum_{j=1}^M \psi_j(x) \psi_j(x') + \sum_{j=M+1}^{N-M} \psi_j(x) \psi_j(x'), \quad (14)$$

For spinless Fermi gas, the single-particle wave functions  $\psi_i(x)$  are also the natural orbitals of the system and  $\lambda_j = 1$ , for  $j = 1, 2, \dots, N$  and all the higher eigenvalues being zero,

$$\rho_1(x, x') = \sum_{i=1}^N \psi_i^*(x) \psi_i(x'), \quad (15)$$

For interacting two-component Fermi gas, we find that interaction leads to significant differences in the spectrum of natural orbitals and their eigenvalues. The populations of lowest six natural orbitals  $\lambda_i(c)$  with the interactions are shown in Fig. 3. We see that the first two natural orbitals ( $i = 1, 2$ ) are dominant and the other higher orbitals ( $i > 2$ ) are separated from them. When the interaction increases, the populations of the lowest two dominant orbitals decreases while those higher orbitals increase slowly. However, the lowest two orbitals are still dominant. We show the profiles of the two dominant natural orbitals for different repulsive interactions

in Fig. 4. In the uncorrelated case  $c = 0$ , the system is in a number state, and natural orbitals coincide with the single-particle eigenstates. When the interaction increases, the natural orbitals will be somewhat distorted but the parity of the orbital is conserved.

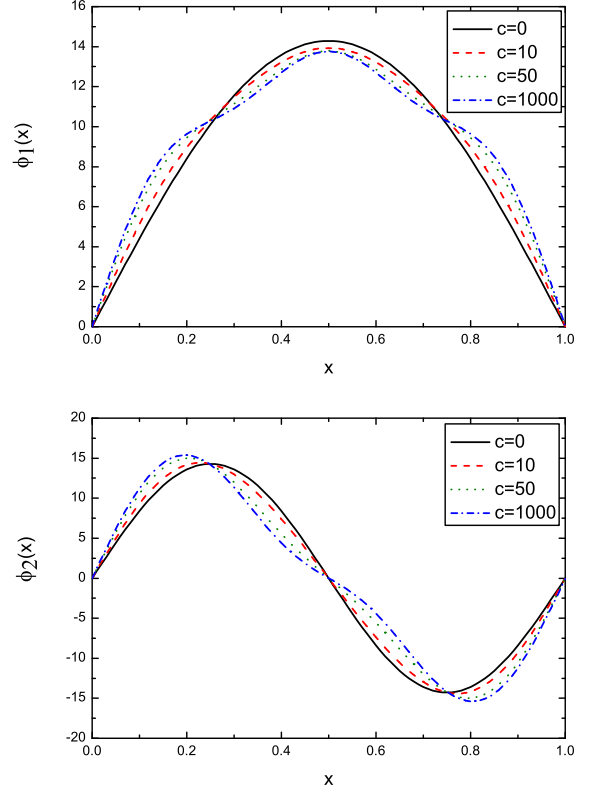


FIG. 4: (color online). The profile of two dominant natural orbitals for different interactions for  $N = 3, M = 1$  fermions.

### C. Momentum density distribution

In experiments, the momentum density distribution detect the off-diagonal correlations of the single-particle reduced density matrix. The momentum density distribution is calculated from the single-particle reduced density matrix

$$n(k) = 2\pi^{-1} \int_0^L dx \int_0^L dx' \rho(x, x') e^{-ik(x-x')}. \quad (16)$$

From Eq. (16), we see that the momentum density distribution  $n(k)$  can be understood as the Fourier transform of the integrated off-diagonal correlation function. Fig. 5 shows the evolution of the momentum density distribution from free fermions to spinless fermions. When the

interaction increases, the distribution becomes smoother, and the half-width becomes larger. When the interaction  $c$  extends to infinity, we find that the momentum density distribution is still different from the spinless fermions although they coincide in real space. This is to be expected as the coordinate exchange symmetry of the two-component fermions is different from that of the spinless fermions.

Comparing with the momentum density distribution of a boson gas in a hard wall trap [13], we see that the momentum density distributions for two-component fermions are smoother and the half-widths are larger. This is due to the Pauli exclusion principle of fermions, that no more than two fermions can occupy same momentum state, so in momentum space the density distributions are broader. For infinite interaction, the hard-core bosons have the same position density as the spinless fermions, but the momentum density distributions are different [13, 21]. The reason is that their wave functions have different symmetry, that is, the wave function of the bosons is symmetric while that of the fermions is antisymmetric.

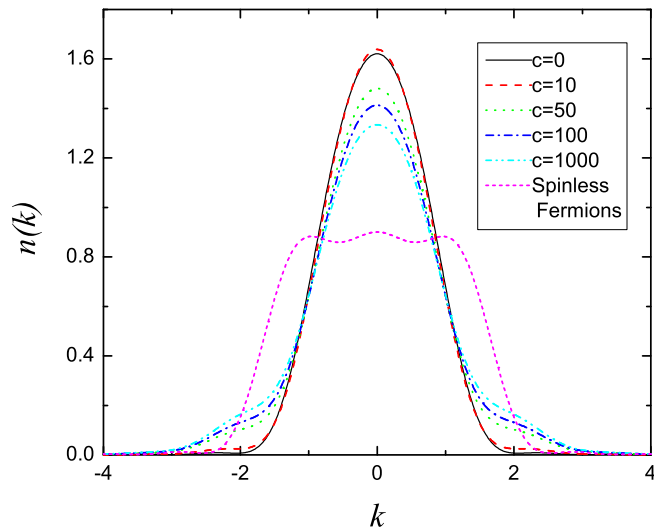


FIG. 5: (color online). Momentum distribution of fermions with different repulsive interactions  $c$  for  $N = 3, M = 1$ .

#### IV. TWO-PARTICLE DENSITY DISTRIBUTION

Now, we consider the two-particle correlations. The two-particle reduced density matrix is  $\rho_2 = \text{tr}_{3\dots N} |\Psi\rangle\langle\Psi|$ . In coordinate representation, the two-particle density, which is the diagonal of the two-particle reduced density matrix, also called the pair distributions, is obtained from the many-body wave function  $\Psi$  as:

$$\rho_2(x_1, x_2) = \frac{N \int_0^L \Psi^*(x_1, x_2, \dots, x_N) \Psi(x_1, x_2, \dots, x_N) dx_3 \dots dx_N}{\int_0^L |\Psi(x_1, x_2, \dots, x_N)|^2 dx_1 \dots dx_N}.$$

The two-particle density expresses the joint probability of finding one particle at position  $x_1$  and any second one at  $x_2$ . We show the two-particle density in Fig. 6 for different interactions. We find that the two-particle density is minimized along the diagonal line for all the interactions due to the Pauli exclusion principle. When the interaction increases, the distributions split into two parts, which demonstrates that the particles are more localized in the well.

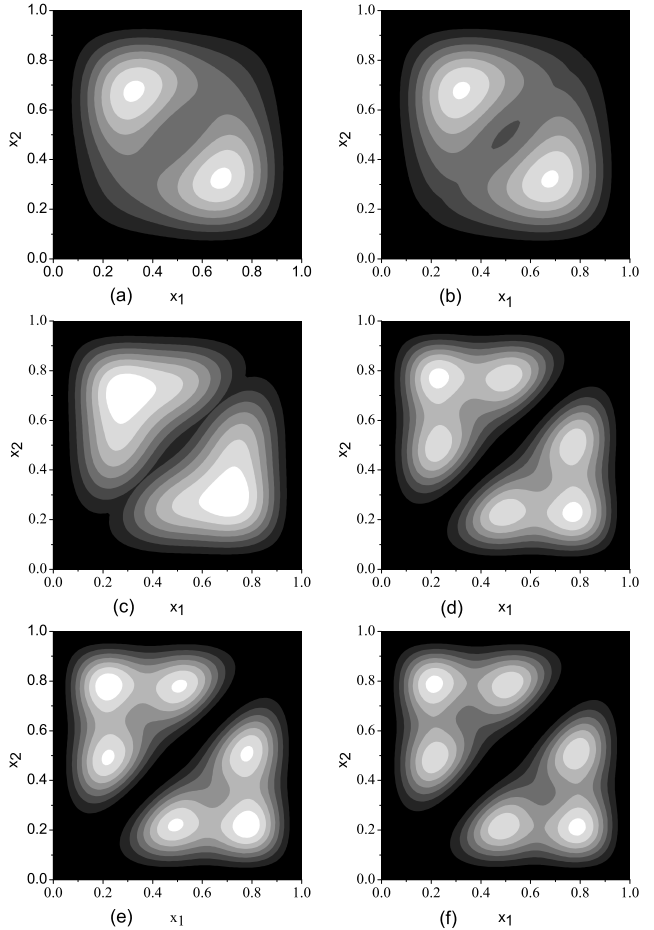


FIG. 6: Two-body density  $\rho(x_1, x_2)$  as a function of interaction strength for three fermions with one down-spin. Shown are the interactions (a)  $c = 0$ , (b)  $c = 1$ , (c)  $c = 10$ , (d)  $c = 50$ , (e)  $c = 100$ , and (f)  $c = 1000$ .

#### V. CONCLUSION

We have investigated the ground state properties of the one-dimensional two-component Fermi gas in an infinite potential well. From the solutions of the Bethe ansatz equations, we obtained the explicit form of the wave function of the system for a few atoms. Then we studied the single-particle reduced density matrix, momentum density distribution and two-particle density matrix for

different interactions. We also found that the momentum density distributions of the strongly interacting two-component fermions were very different from that of the spinless fermions, while the position density distributions of both were the same.

### Acknowledgments

We thanks S. Chen for helpful discussions, and W. L. Chan for the critical reading of our paper. This work is

supported by RGC Grant CUHK 402107, the National Natural Science Foundation of China, and the National Basic Research Programme of China.

- 
- [1] A. Görlitz *et al.*, Phys. Rev. Lett. **87**, 130402 (2001).
  - [2] H. Moritz, T. Stöferle, M. Köhl, and T. Esslinger, Phys. Rev. Lett. **91**, 250402 (2003).
  - [3] T. Kinoshita, T. Wenger, and D. S. Weiss, Science **305**, 1125 (2004).
  - [4] B. Laburthe Tolra, K. M. O'Hara, J. H. Huckans, W. D. Phillips, S. L. Rolston, and J. V. Porto, Phys. Rev. Lett. **92**, 190401 (2004).
  - [5] A. Recati, J. N. Fuchs and W. Zwerger, Phys. Rev. A **71**, 033630 (2005).
  - [6] I. V. Tokatly, Phys. Rev. Lett. **93**, 090405 (2004).
  - [7] M. Olshanii, Phys. Rev. Lett. **81**, 938 (1998).
  - [8] B. E. Granger and D. Blume, Phys. Rev. Lett. **92**, 133202(2004); K. Kanjilal and D. Blume, Phys. Rev. A **70**, 042709(2004).
  - [9] D. S. Petrov, G. V. Shlyapnikov, and J. T. M. Walraven, Phys. Rev. Lett. **85**, 3745 (2000).
  - [10] V. Dunjko, V. Lorent, and M. Olshanii, Phys. Rev. Lett. **86**, 5413 (2001).
  - [11] P. Öhberg, and L. Santos, Phys. Rev. Lett. **89**, 240402 (2002).
  - [12] T. Bergeman, M. G. Moore, and M. Olshanii, Phys. Rev. Lett. **91**, 163201 (2003).
  - [13] Y. J. Hao, Y. B. Zhang, J. Q. Liang, and S. Chen, Phys. Rev. A **73**, 063617 (2006).
  - [14] M. T. Batchelor, X. W. Guan, N. Oelkers, and C. Lee, J. Phys. A **38**, 7787 (2005).
  - [15] M. Gaudin, Phys. Lett. A **24**, 55 (1967).
  - [16] C. N. Yang, Phys. Rev. Lett. **19**, 1312 (1967).
  - [17] F. Woynarovich, Phys. Lett. A. **108**, 401 (1985).
  - [18] N. Oelkers, M. T. Batchelor, M. Bortz and X. W. Guan, J. Phys. A **39**, 1073 (2006).
  - [19] K. Tsujimoto *et al.*, Phys. Lett. A **277**, 123 (2000); T. Shirai *et al.*, Surf. Sci. **514**, 95 (2002).
  - [20] E. Lieb and F. Y. Wu, Phys. Rev. Lett. **20**, 1445 (1968).
  - [21] Y. J. Hao, Y. B. Zhang, and S. Chen, Phys. Rev. A **76**, 063601 (2007).